Fatigue Alleviation by Low-Level Laser Preexposure in Ischemic Neuromuscular Electrical Stimulation

CHIA-CHAN WU[1], YEN-TING LIN[2], CHIA-LING HU[1], YI-CHING CHEN[3,4], and ING-SHIOU HWANG[1,5]

[1]Department of Physical Therapy, College of Medicine, National Cheng Kung University, Tainan City, TAIWAN; [2]Department of Ball Sport, National Taiwan University of Sport, Taichung City, TAIWAN; [3]Department of Physical Therapy, College of Medical Science and Technology, Chung Shan Medical University, Taichung City, TAIWAN; [4]Physical Therapy Room, Chung Shan Medical University Hospital, Taichung City, TAIWAN; and [5]Institute of Allied Health Sciences, College of Medicine, National Cheng Kung University, Tainan City, TAIWAN

ABSTRACT

WU, C.-C., Y.-T. LIN, C.-L. HU, Y.-C. CHEN, and I.-S. HWANG. Fatigue Alleviation by Low-Level Laser Preexposure in Ischemic Neuromuscular Electrical Stimulation. *Med. Sci. Sports Exerc.*, Vol. 56, No. 9, pp. 1795–1804, 2024. **Purpose:** Despite its susceptibility to muscle fatigue, combined neuromuscular electrical stimulation (NMES) and blood flow restriction (BFR) are effective regimens for managing muscle atrophy when traditional resistance exercises are not feasible. This study investigated the potential of low-level laser therapy (LLLT) in reducing muscle fatigue after the application of combined NMES and BFR. **Methods:** Thirty-six healthy adults were divided into control and LLLT groups. The LLLT group received 60 J of 850-nm wavelength LLLT before a training program of combined NMES and BFR of the nondominant extensor carpi radialis longus (ECRL). The control group followed the same protocol but received sham laser therapy. Assessments included maximal voluntary contraction, ECRL mechanical properties, and isometric force tracking for wrist extension. **Results:** The LLLT group exhibited a smaller normalized difference in maximal voluntary contraction decrement (−4.01 ± 4.88%) than the control group (−23.85 ± 7.12%) ($P < 0.001$). The LLLT group demonstrated a smaller decrease in muscle stiffness of the ECRL compared with the control group, characterized by the smaller normalized changes in frequency ($P = 0.002$), stiffness ($P = 0.002$), and relaxation measures ($P = 0.011$) of mechanical oscillation waves. Unlike the control group, the LLLT group exhibited a smaller posttest increase in force fluctuations during force tracking ($P = 0.014$), linked to the predominant recruitment of low-threshold MU ($P < 0.001$) without fatigue-related increases in the discharge variability of high-threshold MU ($P > 0.05$). **Conclusions:** LLLT preexposure reduces fatigue after combined NMES and BFR, preserving force generation, muscle stiffness, and force scaling. The functional benefits are achieved through fatigue-resistant activation strategies of motor unit recruitment and rate coding. **Key Words:** LOW-LEVEL LASER THERAPY, NEUROMUSCULAR ELECTRICAL STIMULATION, BLOOD FLOW RESTRICTION, MOTOR UNITS, ELECTROMYOGRAPHY

In recent years, blood flow restriction (BFR) during exercise, involving the partial restriction of blood flow to working muscles, has gained attention as an effective muscle training approach (1,2). BFR training has various advantages, such as promoting muscle growth with light loads, time-efficient workouts, and convenient use. BFR-induced muscle hypertrophy results from the facilitation of hypoxia-inducible factor 1 (3) or hormone release (4), which are associated with enhanced metabolic stress (5) and cell swelling (6,7). Such ischemic preconditioning also alters muscle activation patterns, causing increases in fast-twitch fiber recruitment (8) and the firing rates of active motor units (MU) (9).

Neuromuscular electrical stimulation (NMES) is a valuable tool for passive muscle training, and it is especially beneficial for individuals who cannot actively participate in traditional resistance training because of injury, surgery, or neuromuscular conditions (10). NMES also induces alterations in muscle activation patterns, characterized by temporal synchrony of MU with spatial invariance and preferential recruitment of fast-twitch muscle fibers (11,12). The stimulation current required for the effective promotion of hypertrophy with NMES is often confined by the patient's pain tolerance (13). The challenge of achieving sufficient contraction levels with NMES can be mitigated if NMES is combined with BFR. This combination has been clinically applied to aid the strength recovery of athletes, elderly individuals, patients with neurological disorders, and so on (14–16). However, BFR leads to the early development of muscle fatigue (17,18), and this fatigability is

Address for correspondence: Ing-Shiou Hwang, Ph.D., Institute of Allied Health Sciences, College of Medicine, National Cheng Kung University, Tainan City 70101, Taiwan; E-mail: ishwang@mail.ncku.edu.tw; Co-Corresponding Author: Yi-Ching Chen, Department of Physical Therapy, College of Medical Science and Technology, Chung Shan Medical University, Taichung City 40201, Taiwan; E-mail: yiching@csmu.edu.tw.

Submitted for publication December 2023.
Accepted for publication April 2024.

0195-9131/24/5609-1795/0
MEDICINE & SCIENCE IN SPORTS & EXERCISE®

DOI: 10.1249/MSS.0000000000003472

multiplied when BFR and NMES are combined. In a previous study by Head et al. (19), it was demonstrated that combining NMES with 80% BFR resulted in a more significant acute force decrement compared with 60% BFR, 40% BFR, and the non-BFR protocol. In addition, the meticulous regulation of force at submaximal contraction intensity allows for the exploration of disruptions in force steadiness underlying impaired recruitment strategies and discharge behaviors of MU (20,21). The ability to precisely control force in submaximal exercises signifies more efficient neuromuscular adaptations after training. This is crucial for optimal movement patterns, improved performance outcomes, and safety in daily activities and athletic pursuits. Neuromuscular fatigue could also impact the mechanical properties of muscles (22). This influence extends to the generation, transmission, and resistance of forces within muscles, closely associated with impairments in muscle activation and contractility (23).

Low-level laser therapy (LLLT) shows promise in reducing muscle fatigue induced by the combination of BFR and NMES. Recent studies have demonstrated that LLLT's photobioenergetic effects can improve performance and prevent neuromuscular fatigue (24,25). These effects are achieved by improving microcirculation, increasing oxygen uptake, and stimulating adenosine triphosphate (ATP) synthesis (26,27). LLLT can also counteract high levels of blood lactate, reactive oxygen species (ROS), and reactive nitrogen species that hinder the binding of calcium ions to myofibrils (28). The application of LLLT could expedite postcontraction recovery after traditional resistance exercise combined with ischemic preconditioning (29). In consideration of the potential energizing effects, this study presents an innovative approach to minimize muscle fatigue after combined NMES and BFR with LLLT preexposure. If the antifatigue effect of preexposure to LLLT is effective, then force generation capacity, mechanical properties of the stimulated muscle, and force precision control will be less affected by combined NMES and BFR. Understanding the antifatigue effect of LLLT can help to optimize the strengthening effect by either increasing the occlusion pressure during BFR or adjusting the training load during NMES. The primary objective was to assess whether LLLT mitigates muscle fatigue induced by the combined intervention of NMES and BFR, ultimately reducing force fluctuations, maintaining maximum strength (maximal voluntary contraction (MVC)) and muscle mechanical properties. Therefore, the following hypotheses were provided: 1) The decline in MVC after the combination of NMES and BFR would be smaller in the subjects who received LLLT than in those who did not receive LLLT. 2) Force scaling and MU activation strategies would be less negatively impacted by the combination of NMES and BFR after preexposure to LLLT. Specifically, preexposure to LLLT was expected to reduce variations in the discharge rate and discharge variability of MU with various recruitment thresholds (R_th) after the combination of NMES and BFR. 3) Finally fatigue-related changes in muscle mechanical properties would be less pronounced in individuals preexposed to LLLT.

METHODS

Subjects. Thirty-six healthy young adults provided informed consent before participating in this study. The experiment received approval from the Institutional Review Board of the National Cheng Kung University Hospital (No. B-ER-111-062). Subjects refrained from vigorous activity and caffeine consumption for 24 h before the experiment. The participants were randomly assigned to one of two gender-balanced groups: control (age: 23.9 ± 2.4 yr; 9 men, 9 women; right-hand dominance: 8 men, 9 women; left-hand dominance: 1 man; height: 167.6 ± 9.0 cm; weight: 65.4 ± 16.9 kg; body mass index: 23.0 ± 4.1 $kg \cdot m^{-2}$) and LLLT (age: 22.6 ± 2.3 yr; 10 men, 8 women; right-hand dominance: 9 men, 8 women; left-hand dominance: 1 man; height: 168.8 ± 8.4 cm; weight: 60.1 ± 12.5 kg; body mass index: 21.0 ± 3.1 $kg \cdot m^{-2}$).

Experimental protocol. On the day of the visit, resting blood pressure was measured with an electric sphygmomanometer (HEM-7121; OMRON Inc., Kyoto, Japan). Participants sat in a chair and relaxed for 3 min before their blood pressure was recorded. After this, they assumed a seated position with their nondominant elbow resting on a wooden platform, slightly flexed at approximately 30 degrees, with their wrist in a pronated position for the baseline measurement. The timeline of the experimental procedure is presented in Figure 1A. Both the pretest and posttest consisted of three measurements: mechanical properties of the extensor carpi radialis longus (ECRL), MVC of wrist extension, and trapezoidal force tracking. Between the pretest and the posttest, a simulated training protocol was conducted using combined NMES and BFR applied to the upper arm. Mechanical properties of the ECRL in the nondominant hand were measured in the middle portion of the muscle belly in both the pretest and posttest stages.

In both the pretest (T1 stage) and posttest (T2 stage), we evaluated force generation capacity and force scaling ability using the MVC and force tracking of wrist extension, respectively. To determine wrist extensor MVC, peak values were recorded with three maximum contraction trials of 3 s, with 1-min rest periods between each trial. After a 3-min rest period after the MVC test, participants performed an isometric trapezoidal force-tracking task (0%–40%–0% MVC) while receiving real-time visual feedback. They were instructed to maintain a static target force of 40% MVC in the middle of the force task (Fig. 1B). The contraction intensity of 40% MVC, empirically determined based on our pilot study, was likely the maximal intensity that permitted all subjects to complete the entire force tracking in the posttest without task failure. This task followed a specific pattern that included a 3-s latent period, a 4-s ramp-up phase to reach 40% of MVC, a 20-v period of maintaining the static force at 40% MVC, a 4-s ramp-down phase to return to rest, and a final 3-s latency period at the end. Each contraction trial lasted a total of 34 s. To focus on the relatively stable force output, the time region of interest (ROI) was defined as the 8th to 26th seconds of each contraction trial. This window allowed for precise analysis of the force-tracking task. The trapezoidal protocol was designed to

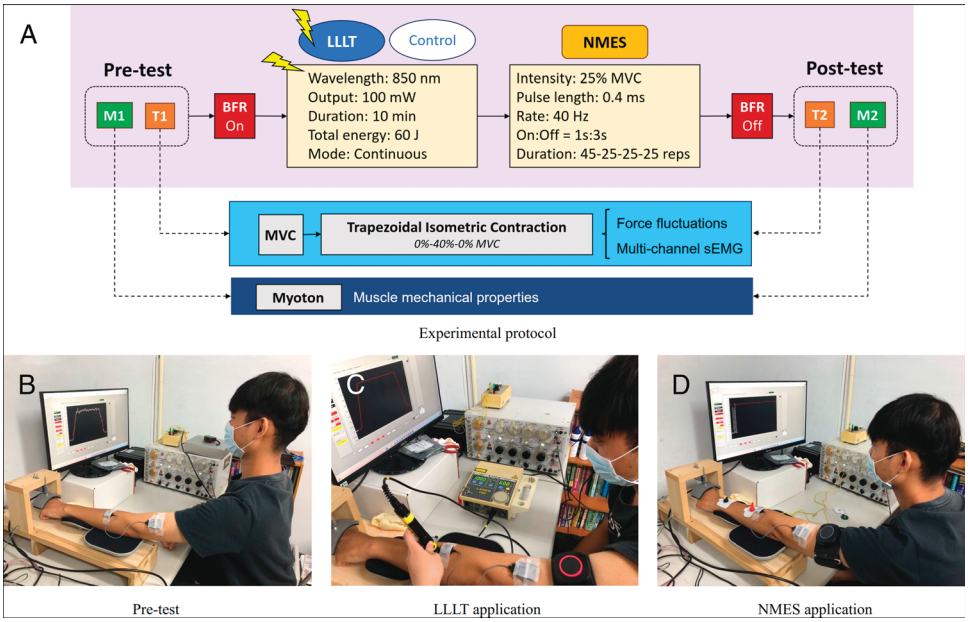

FIGURE 1—(A) Flowchart depicting the experimental process of an NMES intervention involving ischemic and fatigue-preventing preconditioning for the control and LLLT groups. After a 30-s BFR period, LLLT was applied to the muscle belly of ECRL. Subsequently, NMES at 25% MVC, with a pulse length of 0.4 ms, a rate of 40 Hz, and an on/off ratio of 1:3 s, was initiated with a sequence of 45–25–25–25 repetitions, followed by a 30-s rest interval. After this, the BFR was removed. At M1 (pretest) and M2 (posttest), the mechanical properties of the ECRL were measured using the MyotonPRO system. In addition, at T1 (pretest) and T2 (posttest), the force generation capacity and force scaling ability were assessed using an MVC test and a trapezoidal isometric force task (0%–40%–0% MVC), respectively. (B) Surface EMG were placed on the muscle bellies of the ECRL to measure MU during the pretest. (C) Application of LLLT to the muscle belly of the ECRL after 30 s of BFR cuff inflation. (D) A pair of stimulating electrode was placed on the ECRL muscle at the distal part of the forearm during NMES.

facilitate the use of a prevalidated algorithm for electromyography (EMG) decomposition analysis (30). To monitor muscle activity in the ECRL, a four-pin wireless surface EMG electrode was used during the force-tracking task. Each participant completed a total of four trials of trapezoidal contraction, separated by 3-min rest intervals, to assess their force scaling capacity in both the pretest (T1) and posttest (T2).

After the baseline measurements at M1 and T1, we applied wireless auto-calibrating BFR cuffs (SAGA Fitness; SAGA Fitness International, Queensland, Australia) to the biceps brachii muscle belly (Fig. 1C). Venous return in the upper limb was fully obstructed for 10 min with the restriction pressure set at 80% of systolic blood pressure. This ischemic preconditioning technique is known as BFR and facilitates muscle strengthening with NMES under hypoxic conditions. The LLLT group received a 10-min LLLT session, which amounted to a total energy delivery of 60 J. LLLT treatment was administered to the muscle belly of the ECRL (Fig. 1C). In contrast, the control group underwent a sham LLLT treatment. The LLLT system used was a Laser 750 (Electro-Medical Supplies Ltd., Oxon, UK), as utilized in previous studies conducted in our laboratory (29,31). It emitted light at a wavelength of 850 nm with an output power of 100 mW and a spot size of 0.785 cm^2. During the LLLT session, a probe was applied in a stationary and vertical position on the skin over the ECRL muscle.

The subsequent phase involved the application of combined NMES and BFR (Fig. 1D). Pairs of surface electrodes measuring (45 × 30 mm) were affixed to the ECRL muscles located on the back of the nondominant forearm. One of the electrodes was positioned at the same site where the LLLT had earlier been administered, and the other electrode was situated 20 mm proximal to the ulnar styloid process. A stimulator device (S88K; Grass Instruments, Warwick, RI) was employed for the NMES. The stimulus intensity was configured to be 25% of the MVC, with a stimulus rate of 40 Hz and pulse length of 0.4 ms. Each contraction of the stimulated wrist extension lasted for 1 s, followed by a rest period of 3 s. The entire protocol included a total of 120 contraction repetitions of four bouts for the ECRL, organized in a sequence of 45–25–25–25 repetitions, with 30-s rest intervals between bouts. After the NMES session was completed, the occlusion cuff was removed and the participants were allowed to rest for 10 min. The posttest was conducted identically to the pretest.

Instrumentation for physiological measures. The mechanical properties of the ECRL were measured using the MyotonPRO (Myoton AS, Tallinn, Estonia) device (Fig. 2A). The system delivered a mechanical impulse to induce damped oscillations of the muscle and soft tissues of the ECRL. These oscillations were measured using a triaxial accelerometer within the system. Mechanical properties of the ECRL were characterized with oscillation frequency (Hz), dynamic stiffness ($N \cdot m^{-1}$), and relaxation time (ms). Oscillation frequency represented the main sinusoidal wave within the mechanical perturbation waves. Dynamic stiffness ($N \cdot m^{-1}$) represented the tissue's resistance (the first oscillation peak) to external deformation forces. Relaxation time measured the duration for return to its original shape from the first oscillation peak after the removal of an external force (Fig. 2A). The isometric wrist

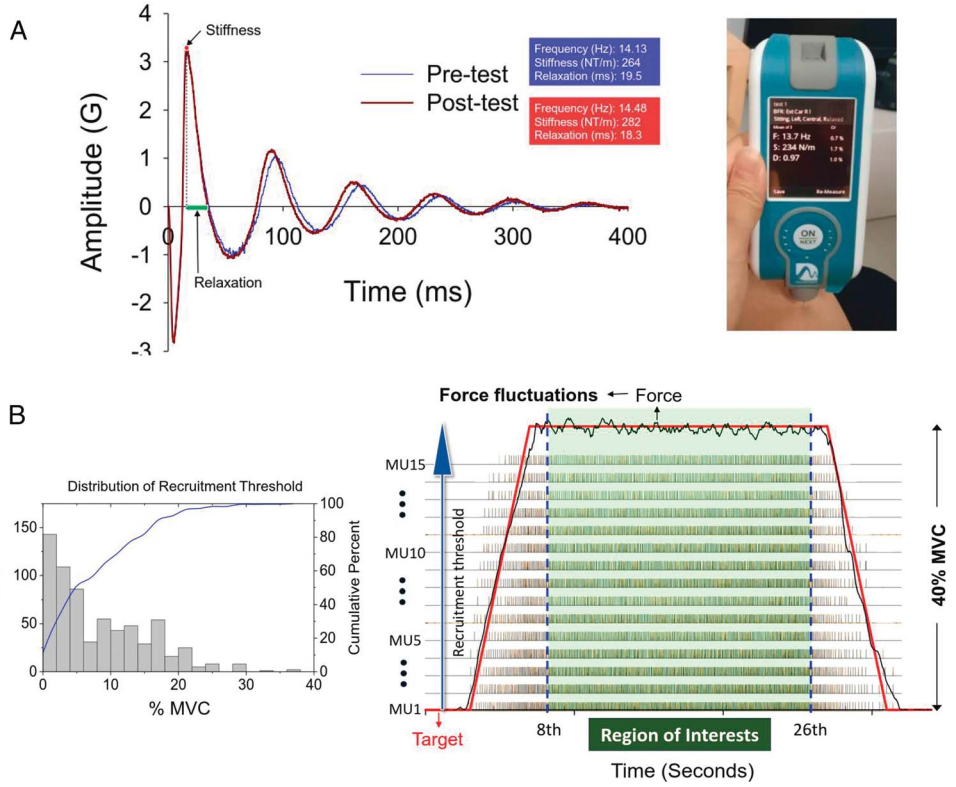

FIGURE 2—(A) The MyotonPRO system and typical perturbation oscillation waves of a control subject in the pretest and posttest. (B) Typical example of surface EMG decomposition results and force trajectory of the force-tracking experiment. Force fluctuations are the force trajectory in the ROI after removal of the linear trend. The spike trains are arranged from bottom to top according to the R_th of the MU. The left plot displays the distribution of recruitment for all MU in the pretest of the control group. Means (M_ISI) and coefficients of variance (CV_ISI) of ISI of individual MU in the ROI were assessed with a single MU action potential train.

extension force was measured using a force sensor (Model: MB-100; Interface Inc., Scottsdale, AZ). The force signal was conditioned through an analog low-pass filter (cut-off frequency: 6 Hz) to eliminate force components unrelated to visuo-motor processes. This filtered force signal was sampled at a rate of 1 kHz with a 16-bit A/D card (USB6251; National Instruments Inc., Austin, TX) on the LabVIEW platform (LabVIEW v.8.5, National Instruments Inc.). For monitoring myoelectrical signals from the ECRL, we utilized a wireless sensor array (Trigno Galileo sensor; Delsys Inc., Natick, MA). The sensor array head (dimensions: 23 × 30 × 7 mm; mass: 19 g) contained four active electrodes arranged in a diamond formation, with an interelectrode distance of 5 mm. The surface electromyography (sEMG) signals of the ECRL were sampled at a rate of 2000 Hz during the force-tracking task, followed by online band-pass filtering (20 to 450 Hz) and streaming to EMG works v.4.7.8 software (Delsys Inc.). Data acquisition for the EMG and force systems was synchronized using a common voltage pulse.

Data analysis. The three variables that represented the mechanical parameters of the ECRL were averaged across trials for each participant. Force fluctuations were the force data within the window of interest (8th to 26th second) after elimination of its linear trend (Fig. 2B). The magnitude of force fluctuations was indexed with the root mean square (RMS) values. NeuroMap v.1.2.1 (Delsys Inc.) was used for the postdecomposition analysis of surface EMG. The four-channel sEMG signals of the entire tracking session were subjected to decomposition, resulting in motor unit action potential waveforms and discharge events (Fig. 2B). Only the spike trains of MU within the window of interest (8th to 26th second) were further analyzed. These decomposition procedures were executed using the software's algorithms (32), which had previously been validated through the decompose–synthesize–decompose–compare method (33,34). In this study, only MU with a decomposition accuracy exceeding 85% using the decompose–synthesize–decompose–compare method were considered for further analysis. This threshold was chosen as a compromise between the 80% criterion established in prior studies (35,36) and the 90% criterion recommended by the EMG system manufacturer (Delsys Inc.) to enable the analysis of as many MU as possible (29). For the pretest and posttest, the decomposition process converted the surface EMG signal from the entire 34-s duration into binary-coded spike trains representing MU with values of either 0 or 1 (Fig. 2B, right). For each MU in the pretest and posttest, interspike intervals (ISI) were averaged to obtain mean ISI (M_ISI) after exclusion of the ISI below 30 ms or above 250 ms, which are scarce during submaximal contractions of the wrist extensors (37,38). Temporal variability of the ISI for a single MU was represented as the coefficient of variation of ISI (CV_ISI). In terms of %MVC, we defined the R_th of an MU as the timing of its initial

discharge during the ramp-up phase of the force tracking (Fig. 2B, left). Signal processing was conducted in Matlab v.2019 (Mathworks Inc., United States).

Statistical analysis. An independent *t*-test was used to analyze the normalized differences ((posttest − pretest)/ pretest × 100%) in mechanical parameters measured by the MyotonPRO system, MVC value, and the size of force fluctuations of the ROI during the force-tracking task between the control and LLLT groups. This study compared differences in MU variables (R_th, M_ISI, and CV_ISI) of pooled MU between the pretest and posttest for the control and LLLT groups. The analysis involved a permutation Hotelling's T^2 test and post hoc permutation paired *t*-test, repeated 10,000 times. Furthermore, this study specified group-dependent variations in discharge behaviors (M_ISI and CV_ISI) of MU of R_th in the ranges of 20% to 40% MVC between the pretest and posttest (5% to 10% of the total number of all identified MU). The emphasis was placed on these MU categories with higher thresholds, as they have the greatest influence on the degree of force fusion and the variability in force production because of their larger twitch forces and slower discharge rates (39). The study also used a permutation Hotelling's T^2 test and post hoc permutation paired *t*-test, repeated 10,000 times, to compare discharge variables (M_ISI and CV_ISI) of MU of high thresholds between the pretest and posttest for the control and LLLT groups. Statistical analyses were performed in the Statistical Package for Social Sciences (SPSS) for Windows version 22.0 and Matlab v.2019 scripts. Data presented in the text and tables are shown as mean ± SD.

RESULTS

Figure 3A presents the normalized differences in MVC between the control and LLLT groups. The results of an independent *t*-test revealed that the posttest decrease in MVC was significantly smaller in the LLLT group (−4.01 ± 4.88%) than in the control group (−23.85 ± 7.12%) ($t_{34} = -9.750$, $P < 0.001$). Figure 3B compares the normalized difference in the RMS of force fluctuations between the control and LLLT groups. The posttest increase in RMS of force fluctuations was significantly smaller in the LLLT group (2.51 ± 19.22%) than in the control group (25.24 ± 31.64%) ($t_{34} = 2.605$, $P = 0.014$). Overall, the control group demonstrated poorer force generation capacity and force precision control than those of the LLLT group after combined NMES and BFR.

The numbers of decomposed MU from multielectrode surface electromyography (EMG) of the ECRL for all participants in the LLLT group during both the pretest and posttest were 815 and 813, respectively. In the control group, the numbers of decomposed MU from the ECRL for all participants

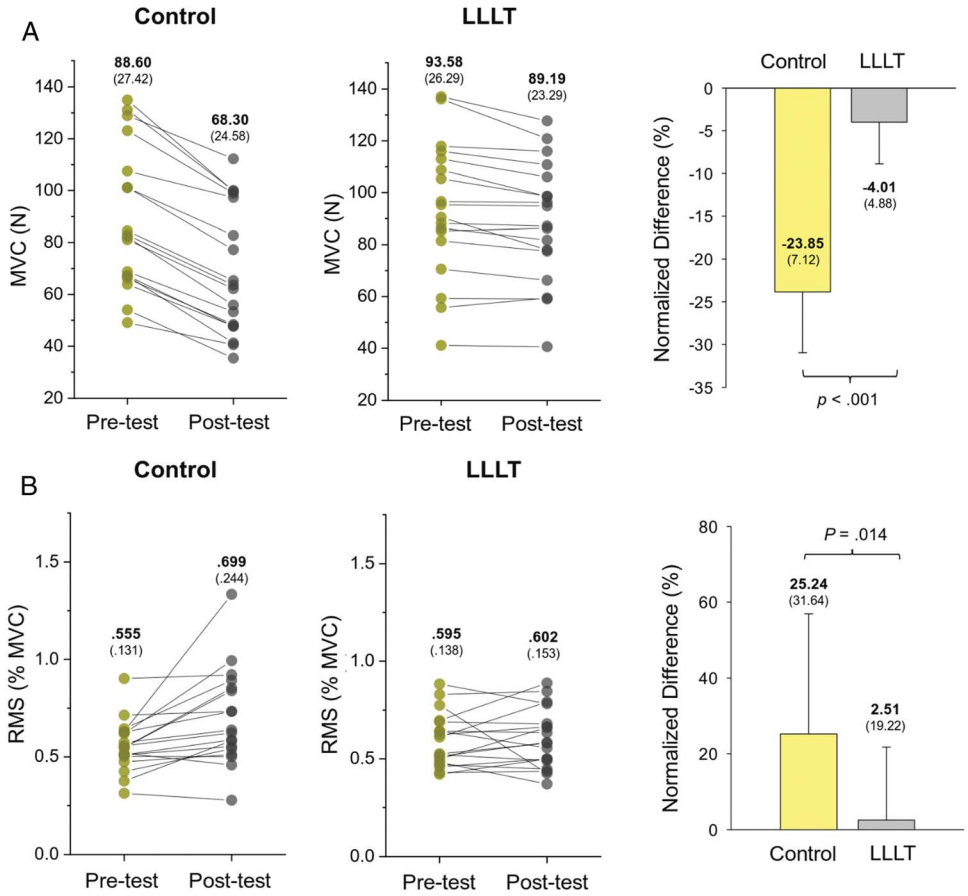

FIGURE 3—The contrast of normalized difference of MVC (A) and force fluctuation parameters (B) between the LLLT and control groups. Means and standard deviations of the force variables in the pretest and posttest are included in the figures.

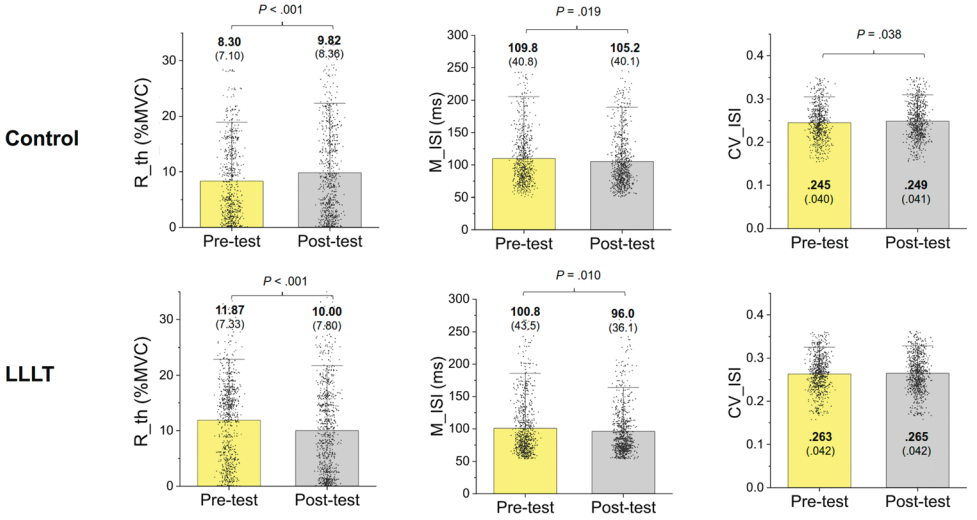

FIGURE 4—The contrast of R_th and discharge patterns of all identified MU between the pretest and posttest for the control and LLLT groups.

during the pretest and posttest were 663 and 738, respectively. Figure 4 illustrates the mean and standard deviations of three main MU variables in the pretest and posttest for the LLLT and control groups. For the control group, the results of the permutation Hotelling's T^2 test indicated significant differences in MU variables between the pretest and posttest ($P < 0.001$). The average R_th of MU was higher in the posttest than in the pretest ($P < 0.001$) (Fig. 4, upper left). The M_ISI was shorter in the posttest than in the pretest ($P = 0.019$) (Fig. 4, upper middle). The coefficient of variation (CV_ISI) was greater in the posttest than in the pretest ($P = 0.038$) (Fig. 4, upper right). For the LLLT group, a permutation Hotelling's T^2 test indicated that MU variables were also significantly different between the pretest and posttest ($P < 0.001$). R_th was smaller in the posttest than in the pretest ($P < 0.001$) (Fig. 4, lower left), oppositely tuned to combined neuromuscular stimulation and BFR in reference to R_th of the control group. As in the control group, M_ISI was smaller in the posttest than in the pretest ($P = 0.010$) (Fig. 4, lower middle). However, contrary to that of the control group, CV_ISI of the LLLT group did not significantly vary between the pretest and posttest ($P >. 05$) (Fig. 4, lower right). Table 1 presents a comparison of M_ISI and CV_ISI for MU with high thresholds (20% to 40% MVC) between the pretest and posttest for both the control and LLLT groups. Only the variables of higher-threshold MU in the control group ($P = 0.001$) changed with combined NMES and BFR. Post hoc analysis revealed that the control group exhibited a shorter M_ISI (pretest: 154.9 ± 43.1 ms, posttest: 138.5 ± 44.9 ms, $P < 0.001$) and greater CV_ISI (pretest: 0.277 ± 0.041, posttest: 0.289 ± 0.033, $P = 0.041$) in the posttest. MU variables of the LLLT group were not significantly affected by combined NMES and BFR ($P > 0.05$).

Table 2 summarizes the posttest-related changes in the mechanical properties of the ECRL muscle between the control and LLLT groups, presenting the normalized differences in various MyotonPRO measures. The results of an independent *t*-test revealed that the posttest frequency decrease in the LLLT group (−0.15 ± 4.05%) was significantly smaller than that in the control group (−5.94 ± 6.02%) ($t_{34} = -3.385$, $P = 0.002$). Furthermore, posttest changes in stiffness were more pronounced in the control group (−7.72 ± 7.17%) than in the LLLT group (0.15 ± 6.74%) ($t_{34} = -3.391$, $P = 0.002$). Finally, the LLLT group exhibited a significantly smaller posttest increase in relaxation (1.57 ± 6.65%) than that in the control group (8.07 ± 7.79%) ($t_{34} = 2.695$, $P = 0.011$). These findings consistently suggest that the mechanical properties of the ECRL muscle were less affected by combined neuromuscular stimulation under the BFR condition in the LLLT group than in the control group.

DISCUSSION

This study demonstrated that preexposure to LLLT produced a photobiomodulation effect for better preservation of MVC, force fluctuation size, and mechanical properties of the working muscle after the application of NMES and BFR. The enhanced precision in force control, resulting from the bioenergetic effect of LLLT, was associated with muscle activation that exhibited prevalent recruitment of MU with lower

TABLE 1. The contrast of discharge patterns of MU with high R_th (20% to 40% MVC) between the pretest and posttest for the control and LLLT groups.

20% to 40% MVC		Pretest	Posttest	Permutation Hotelling's T^2	Post hoc
Control	M_ISI (ms)	**154.9 ± 43.1**	**138.5 ± 44.9**†††	***P* = 0.001**	$P < 0.001$
	CV_ISI	**0.277 ± 0.041**	**0.289 ± 0.033***		$P = 0.041$
LLLT	M_ISI (ms)	144.8 ± 58.9	140.9 ± 55.0	$P = 0.600$	
	CV_ISI	0.285 ± 0.034	0.280 ± 0.037		

*Posttest > pretest, $P < 0.05$; $^{\dagger\dagger\dagger}P < 0.001$.

TABLE 2. The contrast of mechanical properties of ECRL between the LLLT and control groups.

Mechanical Properties		Pretest	Posttest	Normalized Difference (%)	Statistics
Frequency (Hz)	Control	14.29 ± 1.02	13.51 ± 1.01	–5.94 ± 6.02	$t_{34} = -3.385$, $P = 0.002$
	LLLT	13.74 ± 0.73	13.74 ± 0.90	**–0.15 ± 4.05****	
Stiffness ($N \cdot m^{-1}$)	Control	230.50 ± 31.95	212.56 ± 33.52	–7.72 ± 7.17	$t_{34} = -3.391$, $P = 0.002$
	LLLT	211.22 ± 22.37	211.50 ± 25.93	**0.15 ± 6.74****	
Relaxation (ms)	Control	20.38 ± 1.96	21.98 ± 2.16	8.07 ± 7.79	$t_{34} = 2.695$, $P = 0.011$
	LLLT	21.14 ± 1.44	21.49 ± 2.21	**1.57 ± 6.65**‡**	

**LLLT > control, $P < 0.01$; ‡LLLT < control, $P < 0.05$)

thresholds and maintained the discharge stability of MU with higher thresholds.

Preservation of maximal force and muscle stiffness with LLLT preexposure. Previous systematic reviews have shown that LLLT applied before and during exercise can enhance skeletal muscle performance and prevent fatigue (24,40). Both red light (660 nm) and near-infrared (830 nm) are reported to be effective in alleviating muscle fatigue (41). Physiologically, the near-infrared laser, with its longer wavelength, is expected to penetrate deeper into muscle tissues, potentially leading to better outcomes. However, exploration of the antifatigue effect of LLLT on muscle fatigue induced by NMES in humans has been limited (42,43), particularly regarding its potential impact on force precision control and mechanical properties. In fact, the combined application of NMES and BFR is believed to have a more pronounced negative impact on muscle contractility compared with voluntary high-load exercise alone or combined BFR with low-load resistance exercise. This is primarily because BFR-induced high metabolic stress, such as lactate accumulation (44), may compromise central corticospinal excitability (45) and accelerate peripheral muscle fatigue. The fatigability is further deteriorated by concurrent NMES via the induction of lower intracellular pH (46,47) together with the synchronous, spatially fixed recruitment of MU (11,12). These fatigue-related changes and ATP depletion hinder the formation of cross-bridges, resulting in the failure of Ca^{2+} release and ionic changes on the cellular membrane (48–50). Conceptually, our findings align with previous research that has reported the antifatigue effects of photobiomodulation therapy in voluntary exercise (51–53). The bioenergetic effect of LLLT can enhance cytochrome c-oxidase activity (24,42) and upregulate mitochondrial activity within the mitochondrial respiratory chain for enhancement of ATP production within the muscle tissues. Hence, LLLT preexposure provides an ample supply of ATP, which in turn enables the release of Ca^{2+} to counteract the energy crisis induced by the excessive consumption of ATP during the combined application of NMES and BFR. Furthermore, LLLT has the potential to restore ROS homeostasis, which may be disrupted by the combined use of NMES and BFR, thereby maintaining cellular communication pathways mediated by ATP, ROS, and/or calcium (54,55).

The bioenergetic effects of LLLT also contribute to the maintenance of muscle stiffness in the ECRL after the application of combined NMES and BFR (Table 2). Previous studies have shown that acute fatigue induced by prolonged exercise (56,57) or NMES intervention (58) results in a significant decrease in muscle stiffness. This decrease is likely due to the compromise of structural integrity caused by a proinflammatory response (59–61), which leads to increased water content in the connective tissues (62) and reflexive motoneuronal inhibition on muscle elasticity through the activation of III/IV afferents (63,64). It is evident that muscle stiffness after the application of combined NMES and BFR was better preserved with LLLT preexposure, as indicated by relatively insignificant changes in the frequency, stiffness, and relaxation of mechanical oscillation patterns in the ECRL in the posttest (Table 2).

Modulation of MU activation strategy for force precision control with LLLT preexposure. In investigations of the antifatigue effects of LLLT and the impact of BFR on muscle fatigue, only limited attention has been given to examining the force scaling. This gap in research is critical for understanding fine motor control forces, which are interactively regulated by the recruitment strategy and rate coding of MU. In this study, during force tracking, the LLLT group exhibited significantly smaller increases in the RMS of force fluctuations in the posttest compared with the control group (Fig. 3B). Without preexposure to LLLT, the notable rise in force fluctuations observed in the control group suggests the manifestation of neuromuscular fatigue (65). This is related to an increase in discharge variability (Fig. 4, upper right) resulting from shifts in low-frequency common drive to MU (66). In contrast, posttest force steadiness was better preserved, as indicated by insignificant changes in discharge variability in the LLLT group (Fig. 4, lower right). According to the MU model based on computer simulations and experimental data, discharge rate variability is a potent factor negatively influencing isometric force steadiness (67,68). In addition to discharge variability, variations in MU R_th played a crucial role in differentiating force fluctuation performance in the posttest between the control and LLLT groups. In the posttest, the control group exhibited a global increase in R_th (Fig. 4, upper left). This indicates that the control group recruited MU with higher thresholds after the application of combined NMES and BFR. The recruitment of high-threshold MU with larger twitch forces is disadvantageous for achieving smooth force fusion. Collectively, the MU behaviors observed in the control group during the posttest, characterized by higher R_th, shorter ISI, and greater discharge variability (Fig. 4, top row), resembled the typical discharge pattern commonly seen in a fatigued muscle (69,70). In contrast, the R_th in the LLLT group were significantly lower in the posttest (Fig. 4, lower left), indicating that MU with lower thresholds and

twitch forces were predominantly involved in posttest force scaling. Along with shorter ISI to assist smooth force fusion (Fig. 4, bottom row), force fluctuations were not potentiated in the posttest, which supports the beneficial effect of LLLT in resisting neuromuscular fatigue after combined NMES and BFR. In particular, for MU with higher thresholds (20% to 40% of MVC) that play a decisive role in the size of force fluctuations (37), the higher-threshold MU in the LLLT group remained consistent with the application of combined NMES and BFR. In contrast, the higher-threshold MU in the control group displayed fatigue-like discharge behaviors, characterized by increased discharge variability and shorter ISI (Table 1). The scenario provided a rational basis for inferring that these higher-threshold MU were especially responsive to metabolic energy restoration through LLLT (31), contributing to better preservation of force precision control after combined NMES and BFR, although the exact causes warrant further investigations.

Several methodological considerations warrant discussion. First, the relatively small sample size of participants may have limited the representativeness of our study's observations. Nevertheless, this work included 600 to 800 successfully identified MU, a larger set than in most MU studies in this field. The use of the permutation test added statistical robustness for analysis of pooled MU variables. It is valuable to emphasize that this study provides preliminary evidence regarding the positive impact of LLLT irradiation in protecting against the loss of force control and changes in the mechanical properties of the ECRL muscle when combined BFR and NMES is applied. Second, considering MVC and force fluctuation measures (Fig. 3B), few subjects demonstrated an insignificant antifatigue effect on BFR training with LLLT. It is possible that the optimal dose of LLLT for the antifatigue effect could be individualized, despite most positive results being observed with an energy dose range from 20 to 60 J for small muscular groups (25). Third, the composition of the MU investigated may not have been identical between the pretest and posttest. However, it is unlikely that this potential variation significantly impacted the observed MU behaviors, as the EMG electrode remained in position on the recording muscle throughout the relatively short experiment. Last, the precise mechanisms underlying the protective effect of LLLT against neuromuscular fatigue, particularly concerning cellular metabolism and its relationship with force output and MU behaviors, remain incompletely understood.

CONCLUSIONS

This study highlights the potential of LLLT preexposure in mitigating peripheral muscle fatigue when combined with NMES and BFR in terms of force generation capacity, muscle stiffness, and force scaling. The improved force scaling is attributed to the bioenergetic effects of photomodulation, which reduces the strain on MU with lower thresholds and minimizes discharge variability in MU with higher thresholds. LLLT preexposure can help maintain the excitability and discharge stability of MU in the face of fatigue induced by the enhanced metabolic stress and unique MU recruitment patterns associated with combined NMES and BFR. Consequently, LLLT preexposure may be a valuable addition to muscle strengthening protocols involving combined BFR and NMES, allowing for optimization by adjusting training variables such as occlusion pressure and resistance load.

This research was supported by grants from the Ministry of Science and Technology, Taiwan, ROC (MOST 111-2410-H-040-009 and MOST 111-2314-B-006-062-MY3). The authors have no conflict of interest. The results of the study are presented clearly, honestly, and without fabrication, falsification, or inappropriate data manipulation. The results of the present study do not constitute endorsement by the American College of Sports Medicine.

REFERENCES

1. Hughes L, Paton B, Rosenblatt B, Gissane C, Patterson SD. Blood flow restriction training in clinical musculoskeletal rehabilitation: a systematic review and meta-analysis. *Br J Sports Med*. 2017; 51(13):1003–11.
2. Lixandrão ME, Ugrinowitsch C, Berton R, et al. Magnitude of muscle strength and mass adaptations between high-load resistance training versus low-load resistance training associated with blood-flow restriction: a systematic review and meta-analysis. *Sports Med*. 2018; 48(2):361–78.
3. Ferguson RA, Hunt JEA, Lewis MP, et al. The acute angiogenic signalling response to low-load resistance exercise with blood flow restriction. *Eur J Sport Sci*. 2018;18(3):397–406.
4. Reeves GV, Kraemer RR, Hollander DB, et al. Comparison of hormone responses following light resistance exercise with partial vascular occlusion and moderately difficult resistance exercise without occlusion. *J Appl Physiol (1985)*. 2006;101(6):1616–22.
5. Laurentino GC, Ugrinowitsch C, Roschel H, et al. Strength training with blood flow restriction diminishes myostatin gene expression. *Med Sci Sports Exerc*. 2012;44(3):406–12.
6. Loenneke JP, Fahs CA, Rossow LM, Abe T, Bemben MG. The anabolic benefits of venous blood flow restriction training may be induced by muscle cell swelling. *Med Hypotheses*. 2012;78(1): 151–4.
7. Pearson SJ, Hussain SR. A review on the mechanisms of blood-flow restriction resistance training-induced muscle hypertrophy. *Sports Med*. 2015;45(2):187–200.
8. Yasuda T, Brechue WF, Fujita T, Shirakawa J, Sato Y, Abe T. Muscle activation during low-intensity muscle contractions with restricted blood flow. *J Sports Sci*. 2009;27(5):479–89.
9. Fatela P, Mendonca GV, Veloso AP, Avela J, Mil-Homens P. Blood flow restriction alters motor unit behavior during resistance exercise. *Int J Sports Med*. 2019;40(9):555–62.
10. Vinolo-Gil MJ, Rodríguez-Huguet M, Martin-Vega FJ, Garcia-Munoz C, Lagares-Franco C, Garcia-Campanario I. Effectiveness of blood flow restriction in neurological disorders: a systematic review. *Healthcare (Basel)*. 2022;10(12):2407.
11. Gregory CM, Bickel CS. Recruitment patterns in human skeletal muscle during electrical stimulation. *Phys Ther*. 2005;85(4):358–64.
12. Bickel CS, Gregory CM, Dean JC. Motor unit recruitment during neuromuscular electrical stimulation: a critical appraisal. *Eur J Appl Physiol*. 2011;111(10):2399–407.
13. Filipovic A, Kleinöder H, Dörmann U, Mester J. Electromyostimulation—a systematic review of the influence of training regimens and stimulation parameters on effectiveness in electromyostimulation training of selected strength parameters. *J Strength Cond Res*. 2011;25(11): 3218–38.

14. Slysz JT, Boston M, King R, Pignanelli C, Power GA, Burr JF. Blood flow restriction combined with electrical stimulation attenuates thigh muscle disuse atrophy. *Med Sci Sports Exerc*. 2021;53(5):1033–40.
15. Kumaran B, Targett D, Watson T. The effect of an 8-week treatment program using a novel foot neuromuscular electrical stimulator on physical function, leg pain, leg symptoms, and leg blood flow in community-dwelling older adults: a randomized sham-controlled trial. *Trials*. 2022;23(1):873.
16. Gorgey AS, Timmons MK, Dolbow DR, et al. Electrical stimulation and blood flow restriction increase wrist extensor cross-sectional area and flow meditated dilatation following spinal cord injury. *Eur J Appl Physiol*. 2016;116(6):1231–44.
17. de Queiros VS, de França IM, Trybulski R, et al. Myoelectric activity and fatigue in low-load resistance exercise with different pressure of blood flow restriction: a systematic review and meta-analysis. *Front Physiol*. 2021;12:786752.
18. Santiago-Pescador S, Fajardo-Blanco D, López-Ortiz S, et al. Acute effects of electrostimulation and blood flow restriction on muscle thickness and fatigue in the lower body. *Eur J Sport Sci*. 2023;23(8):1591–9.
19. Head P, Waldron M, Theis N, Patterson SD. Acute neuromuscular electrical stimulation (NMES) with blood flow restriction: the effect of restriction pressures. *J Sport Rehabil*. 2020;30(3):375–83.
20. Contessa P, Adam A, De Luca CJ. Motor unit control and force fluctuation during fatigue. *J Appl Physiol (1985)*. 2009;107(1):235–43.
21. Pethick J, Tallent J. The neuromuscular fatigue-induced loss of muscle force control. *Sports (Basel)*. 2022;10(11):184.
22. de Paula Simola RÁ, Harms N, Raeder C, et al. Assessment of neuromuscular function after different strength training protocols using tensiomyography. *J Strength Cond Res*. 2015;29(5):1339–48.
23. Cè E, Longo S, Limonta E, Coratella G, Rampichini S, Esposito F. Peripheral fatigue: new mechanistic insights from recent technologies. *Eur J Appl Physiol*. 2020;120(1):17–39.
24. Nampo FK, Cavalheri V, Dos Santos Soares F, de Paula Ramos S, Camargo EA. Low-level phototherapy to improve exercise capacity and muscle performance: a systematic review and meta-analysis. *Lasers Med Sci*. 2016;31(9):1957–70.
25. Vanin AA, Verhagen E, Barboza SD, Costa LOP, Leal-Junior ECP. Photobiomodulation therapy for the improvement of muscular performance and reduction of muscular fatigue associated with exercise in healthy people: a systematic review and meta-analysis. *Lasers Med Sci*. 2018;33(1):181–214.
26. Leal Junior ECP, Lopes-Martins RAB, Dalan F, et al. Effect of 655-nm low-level laser therapy on exercise-induced skeletal muscle fatigue in humans. *Photomed Laser Surg*. 2008;26(5):419–24.
27. Hayworth CR, Rojas JC, Padilla E, Holmes GM, Sheridan EC, Gonzalez-Lima F. In vivo low-level light therapy increases cytochrome oxidase in skeletal muscle. *Photochem Photobiol*. 2010;86(3):673–80.
28. Moopanar TR, Allen DG. Reactive oxygen species reduce myofibrillar Ca2+ sensitivity in fatiguing mouse skeletal muscle at 37°C: reactive oxygen species and muscle fatigue. *J Physiol*. 2005;564(1):189–99.
29. Chen YC, Lin YT, Hu CL, Hwang IS. Low-level laser therapy facilitates postcontraction recovery with ischemic preconditioning. *Med Sci Sports Exerc*. 2023;55(7):1326–33.
30. De Luca CJ, Chang SS, Roy SH, Kline JC, Nawab SH. Decomposition of surface EMG signals from cyclic dynamic contractions. *J Neurophysiol*. 2015;113(6):1941–51.
31. Chen YC, Su YH, Lin YT, Huang CC, Hwang IS. Acute physiological responses to combined blood flow restriction and low-level laser. *Eur J Appl Physiol*. 2020;120(6):1437–47.
32. De Luca CJ, Contessa P. Biomechanical benefits of the onion-skin motor unit control scheme. *J Biomech*. 2015;48(2):195–203.
33. De Luca CJ, Adam A, Wotiz R, Gilmore LD, Nawab SH. Decomposition of surface EMG signals. *J Neurophysiol*. 2006;96(3):1646–57.
34. De Luca CJ, Contessa P. Hierarchical control of motor units in voluntary contractions. *J Neurophysiol*. 2012;107(1):178–95.
35. Madarshahian S, Latash ML. Synergies at the level of motor units in single-finger and multi-finger tasks. *Exp Brain Res*. 2021;239(9):2905–23.
36. Madarshahian S, Letizi J, Latash ML. Synergic control of a single muscle: the example of flexor digitorum superficialis. *J Physiol*. 2021;599(4):1261–79.
37. Palmer SS, Fetz EE. Discharge properties of primate forearm motor units during isometric muscle activity. *J Neurophysiol*. 1985;54(5):1178–93.
38. Romaiguère P, Vedel JP, Pagni S, Zenatti A. Physiological properties of the motor units of the wrist extensor muscles in man. *Exp Brain Res*. 1989;78(1):51–61.
39. Contessa P, De Luca CJ. Neural control of muscle force: indications from a simulation model. *J Neurophysiol*. 2013;109(6):1548–70.
40. Alves AN, Fernandes KPS, Deana AM, Bussadori SK, Mesquita-Ferrari RA. Effects of low-level laser therapy on skeletal muscle repair: a systematic review: a systematic review. *Am J Phys Med Rehabil*. 2014;93(12):1073–85.
41. de Almeida P, Lopes-Martins RAB, De Marchi T, et al. Red (660 nm) and infrared (830 nm) low-level laser therapy in skeletal muscle fatigue in humans: what is better? *Lasers Med Sci*. 2012;27(2):453–8.
42. Gorgey AS, Wadee AN, Sobhi NN. The effect of low-level laser therapy on electrically induced muscle fatigue: a pilot study. *Photomed Laser Surg*. 2008;26(5):501–6.
43. Jówko E, Płaszewski M, Cieśliński M, Sacewicz T, Cieśliński I, Jarocka M. The effect of low level laser irradiation on oxidative stress, muscle damage and function following neuromuscular electrical stimulation. A double blind, randomised, crossover trial. *BMC Sports Sci Med Rehabil*. 2019;11(1):38.
44. Cayot TE, Lauver JD, Silette CR, Scheuermann BW. Effects of blood flow restriction duration on muscle activation and microvascular oxygenation during low-volume isometric exercise. *Clin Physiol Funct Imaging*. 2016;36(4):298–305.
45. Peyrard A, Willis SJ, Place N, Millet GP, Borrani F, Rupp T. Neuromuscular evaluation of arm-cycling repeated sprints under hypoxia and/or blood flow restriction. *Eur J Appl Physiol*. 2019;119(7):1533–45.
46. Vanderthommen M, Duteil S, Wary C, et al. A comparison of voluntary and electrically induced contractions by interleaved 1H- and 31P-NMRS in humans. *J Appl Physiol (1985)*. 2003;94(3):1012–24.
47. Theurel J, Lepers R, Pardon L, Maffiuletti NA. Differences in cardiorespiratory and neuromuscular responses between voluntary and stimulated contractions of the quadriceps femoris muscle. *Respir Physiol Neurobiol*. 2007;157(2–3):341–7.
48. Allen DG, Westerblad H. Role of phosphate and calcium stores in muscle fatigue. *J Physiol*. 2001;536(3):657–65.
49. Allen DG, Lamb GD, Westerblad H. Skeletal muscle fatigue: cellular mechanisms. *Physiol Rev*. 2008;88(1):287–332.
50. Cairns SP, Inman LAG, MacManus CP, et al. Central activation, metabolites, and calcium handling during fatigue with repeated maximal isometric contractions in human muscle. *Eur J Appl Physiol*. 2017;117(8):1557–71.
51. Antonialli FC, De Marchi T, Tomazoni SS, et al. Phototherapy in skeletal muscle performance and recovery after exercise: effect of combination of super-pulsed laser and light-emitting diodes. *Lasers Med Sci*. 2014;29(6):1967–76.
52. Vanin AA, De Marchi T, Tomazoni SS, et al. Pre-exercise infrared low-level laser therapy (810 nm) in skeletal muscle performance and postexercise recovery in humans, what is the optimal dose? A randomized, double-blind, placebo-controlled clinical trial. *Photomed Laser Surg*. 2016;34(10):473–82.
53. Silva M, Gáspari A, Barbieri J, et al. Far-infrared-emitting fabric improves neuromuscular performance of knee extensor. *Lasers Med Sci*. 2022;37(5):2527–36.
54. Reid MB. Free radicals and muscle fatigue: of ROS, canaries, and the IOC. *Free Radic Biol Med*. 2008;44(2):169–79.

55. Xu X, Zhao X, Liu TCY, Pan H. Low-intensity laser irradiation improves the mitochondrial dysfunction of C2C12 induced by electrical stimulation. *Photomed Laser Surg*. 2008;26(3):197–202.
56. Kim DH, Jung YJ, Song YE, Hwang DH, Ko CY, Kim HS. 1C5–1 measurement of characteristic change using MyotonPRO in low back muscles during a long-term driving; Pilot study. *Jpn J Ergon*. 2015; 51(Supplement):S450–3.
57. Andonian P, Viallon M, Le Goff C, et al. Shear-wave elastography assessments of quadriceps stiffness changes prior to, during and after prolonged exercise: a longitudinal study during an extreme mountain ultra-marathon. *PLoS One*. 2016;11(8):e0161855.
58. Sheng Z, Sharma N, Kim K. Quantitative assessment of changes in muscle contractility due to fatigue during NMES: an ultrasound imaging approach. *IEEE Trans Biomed Eng*. 2020;67(3):832–41.
59. Kjaer M, Magnusson P, Krogsgaard M, et al. Extracellular matrix adaptation of tendon and skeletal muscle to exercise. *J Anat*. 2006; 208(4):445–50.
60. Millet GY, Tomazin K, Verges S, et al. Neuromuscular consequences of an extreme mountain ultra-marathon. *PLoS One*. 2011;6(2):e17059.
61. Hjorth M, Norheim F, Meen AJ, et al. The effect of acute and long-term physical activity on extracellular matrix and serglycin in human skeletal muscle. *Physiol Rep*. 2015;3(8):e12473.
62. Proske U, Morgan DL. Muscle damage from eccentric exercise: mechanism, mechanical signs, adaptation and clinical applications. *J Physiol*. 2001;537(2):333–45.
63. Avela J, Kyröläinen H, Komi PV, Rama D. Reduced reflex sensitivity persists several days after long-lasting stretch-shortening cycle exercise. *J Appl Physiol (1985)*. 1999;86(4):1292–300.
64. Regueme SC, Nicol C, Barthèlemy J, Grélot L. Acute and delayed neuromuscular adjustments of the triceps surae muscle group to exhaustive stretch-shortening cycle fatigue. *Eur J Appl Physiol*. 2005; 93(4):398–410.
65. Huang CT, Hwang IS, Huang CC, Young MS. Exertion dependent alternations in force fluctuation and limb acceleration during sustained fatiguing contraction. *Eur J Appl Physiol*. 2006;97(3):362–71.
66. Hwang IS, Lin YT, Huang CC, Chen YC. Fatigue-related modulation of low-frequency common drive to motor units. *Eur J Appl Physiol*. 2020;120(6):1305–17.
67. Enoka RM, Christou EA, Hunter SK, et al. Mechanisms that contribute to differences in motor performance between young and old adults. *J Electromyogr Kinesiol*. 2003;13(1):1–12.
68. Moritz CT, Barry BK, Pascoe MA, Enoka RM. Discharge rate variability influences the variation in force fluctuations across the working range of a hand muscle. *J Neurophysiol*. 2005;93(5):2449–59.
69. De Luca CJ, Hostage EC. Relationship between firing rate and recruitment threshold of motoneurons in voluntary isometric contractions. *J Neurophysiol*. 2010;104(2):1034–46.
70. Stock MS, Beck TW, Defreitas JM. Effects of fatigue on motor unit firing rate versus recruitment threshold relationships: motor unit fatigue. *Muscle Nerve*. 2012;45(1):100–9.